Theoretical estimations of the efficiency of thermophotovoltaic systems using high-intensity silicon solar cells

Article *in* Solar Energy · December 1984

DOI: 10.1016/0038-092X(84)90046-X

CITATIONS
8

READS
16

2 authors, including:

José Luis Duomarco
A.I.U.
30 PUBLICATIONS **19** CITATIONS

SEE PROFILE

Solar Energy, Vol. 32, No. 1, pp. 33–40, 1984
Printed in Great Britain.

0038-092X/84 $3.00 + .00

THEORETICAL ESTIMATIONS OF THE EFFICIENCY OF THERMOPHOTOVOLTAIC SYSTEMS USING HIGH-INTENSITY SILICON SOLAR CELLS†

JOSE L. DUOMARCO‡ and ROY KAPLOW
Department of Materials Science and Engineering, Massachusetts Institute of Technology, Cambridge, MA 02139, U.S.A.

(*Received* 4 *April* 1982)

Abstract—Efficiencies have been calculated for (a) heat-mirror filter and (b) rear-mirror thermophotovoltaic systems using actual materials values for source emissivity ($\epsilon(\lambda)$), mirror-filter transmissivity ($\tau_M(\lambda)$) and intensity-dependent cell parameters V_{oc} and FF. The ratios of heat-mirror and rear-mirror efficiencies to direct sunlight impingement efficiency are estimated to be 1.6 and 1.9, respectively (2500°K thermal source), if mirror and other extraneous absorption are taken to be zero in both cases. The more realistic inclusion, for the first case, of 2 per cent light absorption in the filter/mirror and, in the second case, of 2 per cent absorption of low energy light in the cell and 8 per cent absorption at the rear mirror, plus a 2 per cent thermal loss directly from the hot source (for both), reduces the advantage of both to about a factor of 1.2.

INTRODUCTION

The sunlight concentration–thermophotovoltaic approach to solar energy conversion[1–3] allows control of the spectral characteristics of the radiation incident on the photovoltaic cell, conservation of low energy radiation which would otherwise be converted to "waste" heat, and control of the intensity level—which also affects conversion efficiency.

The major energy losses in photovoltaic cell conversion to electricity are associated with the excess energy in photons more energetic than necessary to excite an electron-hole pair and the total energy in photons less energetic than necessary. If $N(E)\,dE$ is the number of incident photons in an energy interval, and E_{gap} the energy necessary to create an electron-hole pair of electrical carriers, the energy unavailable for direct electrical conversion is

$$\int_0^{E_{gap}} N(E)E\,dE + \int_{E_{gap}}^{\infty} N(E)(E - E_{gap})\,dE. \quad (1)$$

For silicon under AM1 solar illumination this amounts to 51.4 per cent of the total.

In this report we examine, by computer modeling, the effectiveness of using a hot source (e.g. heated by concentrated sunlight) with selective emissivity and a "heat mirror" type of filter. The principle of such a system is to improve the operational efficiency by generating and passing to the cell photons which are higher than E_{gap} (but not excessively higher) while reflecting photons below E_{gap} back to the hot source. Such a system is shown in Fig. 1. The calculations are also applicable to a variation of the system in which a mirror on the rear side of the photocells reflects unabsorbed photons (generally those with $E < E_{gap}$) back to the source[4]. Figure 1 can also serve for the latter configuration, by removing the heat-mirror (c) and imagining the cell rear surface metallization (e) to be a highly reflecting surface.

Concentrated solar radiation is focussed into the device through an aperature (Figure 1(a)) and is absorbed by the thermal source (b) in the core of the evacuated cavity. The aperture is small compared to the 2π solid angle. The source reaches an "equilibrium" temperature T, emitting a radiation spectrum determined by T and the emissivity, $\epsilon(\lambda)$, of its surface. Radiation emitted towards the cell is transmitted through a heat mirror (c) with a characteristic transmissivity $\tau_M(\lambda)$. The transmitted radiation is collected by high-intensity solar cells (d) which are maintained at a relatively low temperature with the aid of a coolant (f) in a cooling jacket (g) in the exterior layer. The cells are maintained at lower or higher temperature,

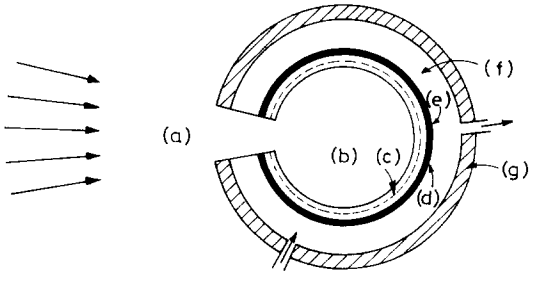

Fig. 1. Schematic of heat-mirror thermophotovoltaic device: (a) solar aperture, (b) selective emissivity absorber-radiator core, (c) mirror-filter, (d) solar cells, (e) rear metallization, (f) coolant, (g) insulated jacket.

†This work was sponsored in part by the M.I.T./Cabot Solar Energy Fund.

‡Fulbright-Fletcher Fellow, 1979–1980. Present address: Instituto de Física, Facultad de Ingeniería, Universidad de la República, Montevideo, Uruguay.

depending on the temperature coefficient of cell efficiency and the utility and value of the low temperature thermal energy as a function of its temperature. If the efficiency of the device is adequate, it has the advantage that the thermal source can be heated with auxiliary fuel when necessary on sunless occasions. Desirable spectral characteristics for source emissivity and the filter transmissivity minimize the integral of eqn (1). Overall efficiency is also dependent on the mirror absorptivity, $\alpha_M(\lambda)$, weighted in accordance with the source emissivity as well as other "non-idealities".

The digital computer models provide an economic means of testing the joint effect of different materials and configurations. Although we have used idealizations to introduce simplifications and for comparative purposes, a major point of the current work has been to use the real properties of photovoltaic cells and of selected materials where possible. For simplicity, we have taken the photocell area to be the same as that of the thermal source. That is, there is no internal de-concentration. If desired, a correction can be applied to the cell efficiency for a particular geometric configuration, depending only on the intensity dependent cell characteristics, which vary slowly with intensity.

DESCRIPTION OF THE COMPUTER MODEL

The thermal source (b), at temperature T, emits balckbody radiation modified by the spectral emissivity, $\epsilon(\lambda)$, of its surface and by the transmission distribution of the mirror filter, $\tau_M(\lambda)$. The solar cell surface has an anti-reflectance coating with transmission, $\tau_{AR}(\lambda)$, and a spectral quantum yield, $S(\lambda)$ (electrons/photon). Where it has been relevant to introduce detailed cell behavior, we have referred to data on etched multiple vertical junction (EMVJ) high-intensity cells [5]. Experimental values have been used for $S(\lambda)$† and for the open circuit voltage (V_{oc}) and the fill factor (FF) [6], either as a function of intensity or as the fixed value corresponding to 500 suns concentration.

The light intensity (W/m^2) reaching the photocells' surface is given by the following formula [7–9]

$$P_s(T, 0 < \lambda < \infty, \epsilon(\lambda), \tau_M(\lambda)) = \frac{15}{\pi^4}\sigma\left(\frac{hc}{k}\right)^4 \int_0^\infty \frac{\epsilon(\lambda)\tau_M(\lambda)\,d\lambda}{\lambda^5(e^{(hc/kT\lambda)} - 1)}. \quad (2)$$

Taking into account the antireflectance coating (AR), the current density (A/m^2) generated in the photocells is given by:

$$J_s(T, 0 < \lambda < \infty, \epsilon(\lambda), \tau_M(\lambda), \tau_{AR}(\lambda), S(\lambda)) = \frac{15}{\pi^4} \times \sigma\left(\frac{hc}{k}\right)^4 \times \int_0^\infty \frac{\epsilon(\lambda)\tau_M(\lambda)\tau_{AR}(\lambda)}{\lambda^5(e^{(hc/kT\lambda)} - 1)} \cdot \frac{S(\lambda)q\lambda\,d\lambda}{hc}. \quad (3)$$

†The $S(\lambda)$ function pertains to a cell thickness of about 0.02 cm.

The electrical efficiency of the photocells at maximum power output includes the intensity-dependent variables, fill factor (FF) and open circuit voltage (V_{oc}) and is given by the following formula:

$$\eta_s(T) = \frac{J_s(T, 0 < \lambda < \infty, \epsilon, \tau_M, \tau_{AR}, S) \cdot FF(P_s) \cdot V_{oc}(P_s)}{P_s(T, 0 < \lambda < \infty, \epsilon, \tau_M)} \cdot 100. \quad (4)$$

We also calculated two purely theoretical efficiencies given by the following formulae:

$$\eta_0(T) = \frac{J_0(T, 0 < \lambda < \lambda_{gap}) \cdot FF(P_s) \cdot V_{oc}(P_s)}{P_0(T, 0 < \lambda < \infty)} \cdot 100. \quad (5)$$

$$\eta_f(T) = \frac{J_0(T, 0 < \lambda < \lambda_{gap}) \cdot FF(P_s) \cdot V_{oc}(P_s)}{P_f(T, 0 < \lambda < \lambda_{gap})} \cdot 100. \quad (6)$$

These latter two define an idealized range for reference. The first (eqn 5) corresponds to having a thermal source with a uniform emissivity of 1.0, no heat mirror, and a cell with a perfect anti-reflection coating and perfect quantum efficiency for photons above E_{gap}. The second differs by having a perfect heat mirror which allows only electron-hole pair producing photons to pass; in the limit this idealization yields 100 per cent efficiency when the temperature cut off limit coincides with E_{gap}, albeit with effectively zero power output.

Calculations were done (as in eqn 4) using the published characteristics of an actual heat mirror [10]. In addition, since it would appear to be feasible to slightly move the "cutoff" position of a multilayer mirror filter [11], we also ran through an optimization procedure, translating the filter's spectral transmission distribution function $\tau_M(\lambda)$ into $\tau_M(\lambda + x)$. A detailed study of $P_s(T, x)$, $J_s(T, x)$ and $\eta_s(T, x)$ was done to seek an optimum location for the filter's pass band.

A dual criterion for optimization results: maximum electrical current density for a given source temperature or maximum efficiency, since one condition does not necessarily imply the other.

The source temperature is of main importance, within the framework of this study, through its effect on the spectral characteristics of the radiation. Since the power radiation law is a function of temperature (σT^4), the temperature of operation also determines the radiation intensity and thus the total electrical power output, and—as alluded to above—also the electrical conversion efficiency. It is, therefore, important to note that the basic calculations were done on a fixed area of source basis. Certain of the electrical conversion efficiency comparisons were renormalized, however, so as to remove the effect of intensity variations among particular comparisons.

RESULTS

For this work we have used the published characterization data for a silicon EMVJ photocell developed recently[6]. The cell design has only a small internal series resistance, with the result that the efficiency increases with increasing intensity up to perhaps 500 suns; it is thus particularly suitable for high concentration. The open circuit voltage V_{oc} and the fill factor FF, are shown in Fig. 2 and the quantum yield used, $S(\lambda)$, is shown in Fig. 3. The presumed antireflecting (AR) coating is a double-layer coating on silicon that reduces the reflection to around 3 per cent averaged over the silicon cell response range in sunlight (0.4–1.1 μm)[12]. Its transmission distribution function, $\tau_{AR}(\lambda)$, is shown in Fig. 3.

The thermal source (or its surface) is assumed to be aluminum oxide (sapphire) with an emissivity $\epsilon(\lambda)$ shown in Fig. 4[13].

No term has been included explicitly for photocell area obscured by contacts, but the light reflected by such areas will mostly be retrieved by the source.

The heat mirror is a composite $TiO_2/Ag/TiO_2$ film, designed for solar application, and with a transmission spectral function $\tau_M(\lambda)$ shown in Fig. 4[10]. Variation of the film's thickness or of the index of refraction of the dielectric layers can change the location of the passband frequency[11]. The product function, $\tau_M(\lambda + x) \cdot \epsilon(\lambda)$, which modifies the blackbody spectrum, is shown in Fig. 5 for several values of the parameter x. The light intensity $P_s(T, x)$, the current density $J_s(T, x)$ and the electrical efficiency $\eta_s(T, x)$ are shown in Figs. 6–8, respectively. The locus of optimum x is shown on all three of these. The optimum efficiency occurs near $x = +0.35$ for all temperatures ≥ 1500K and that value also yields near maximum J_s (within 10 per cent). For that shift, the pass-band peak of the mirror is at $\lambda = 0.80\,\mu$m.

The temperature dependence of the light intensity, P_s, is shown in Fig. 9 for $x = 0.0$ and $x = +0.35$. In Fig. 10 we show the corresponding J_s for the $x = 0.0$, $x = +0.35$ and true optimum sections. Although the spectral characteristics are different from sunlight, of

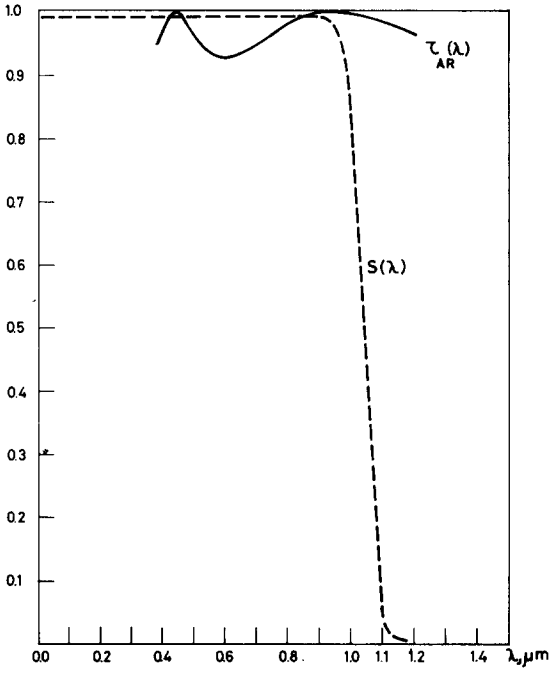

Fig. 3. Spectral quantum yield, $s(\lambda)$ (electrons/photon), and anti-reflectance coating transmissivity, $\tau_{AR}(\lambda)$ (per cent/100), Refs. [5, 12].

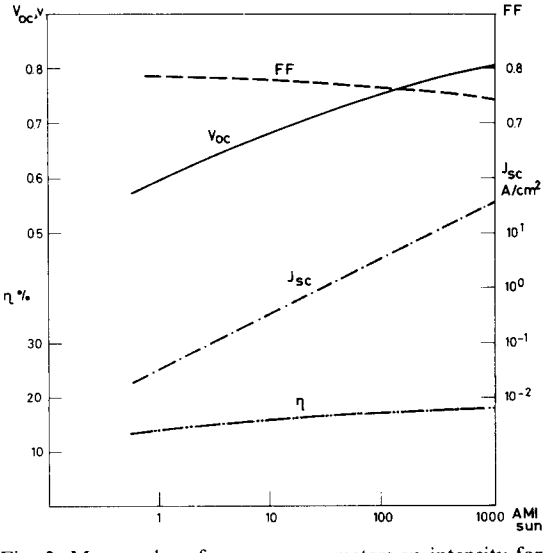

Fig. 2. Measured performance parameters vs intensity for 0.64 cm EMVJ square cells with oxide AR coating (at 27°C), Ref. [6].

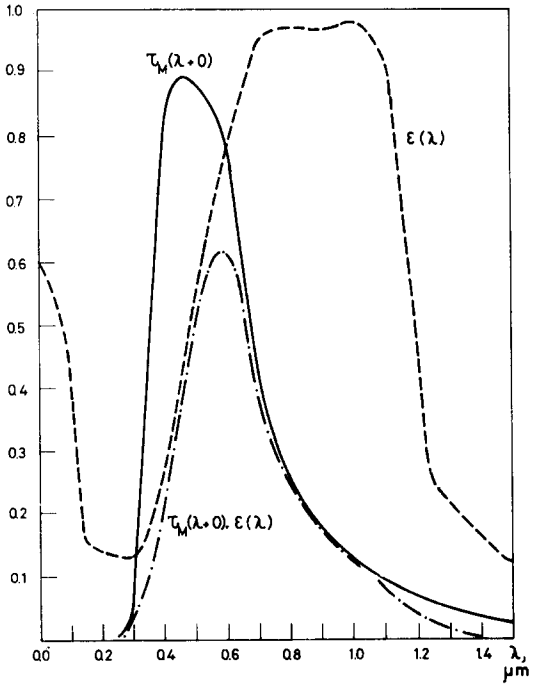

Fig. 4. Spectral emittance of aluminum oxide (sapphire), $\epsilon(\lambda)$ (per cent/100); transmission of a 180 A TiO_2/180 A Ag/180 A TiO_2 film on glass (~1 mm thick) $\tau_m(\lambda)$ (per cent/100), and Refs. [13, 10].

course, it is worth recalling that unconcentrated peak sunlight is approximately 10^3 W/m^2; therefore, for the temperature range covered in Figs. 9 and 10 (1500–5500K), we are dealing with intensities ranging from a few suns to 10^4 suns. At, say, 2500K the intensity level for $x = 0.35$ is ~ 300 suns.

In Fig. 11, we show cell efficiency curves as a

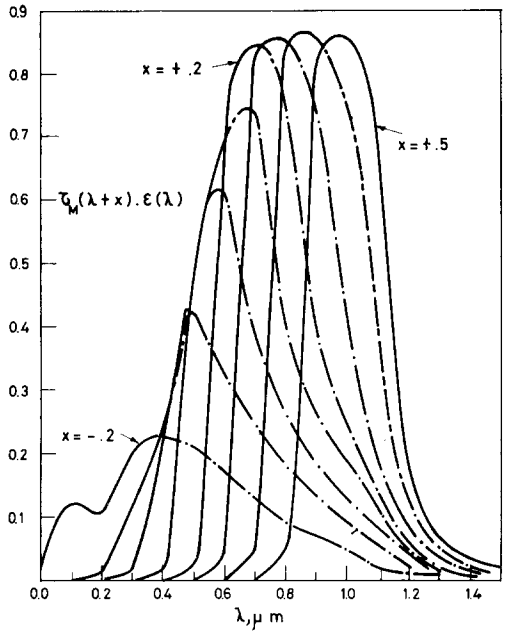

Fig. 5. Blackbody radiation factor $\tau(\lambda + x)\cdot\epsilon(\lambda)$ for $x = -0.2$, 0.1, 0.0, 0.1, 0.2, 0.3, 0.4 and 0.5 μm.

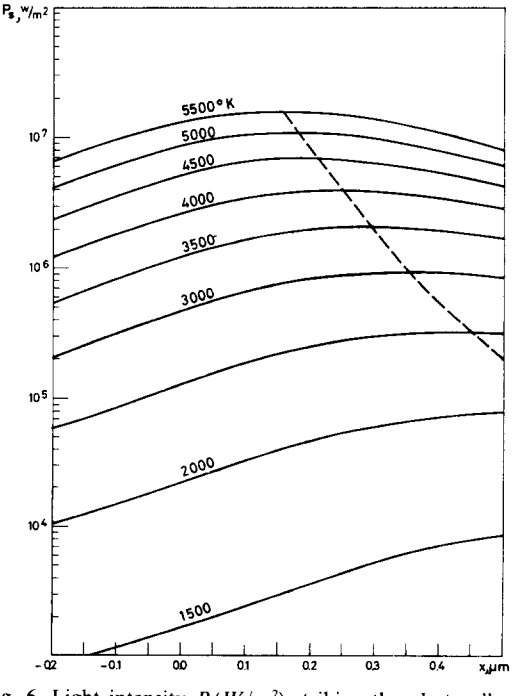

Fig. 6. Light intensity $P_s(W/m^2)$ striking the photocell as function of temperature (°K) and filter pass band displacement (μm).

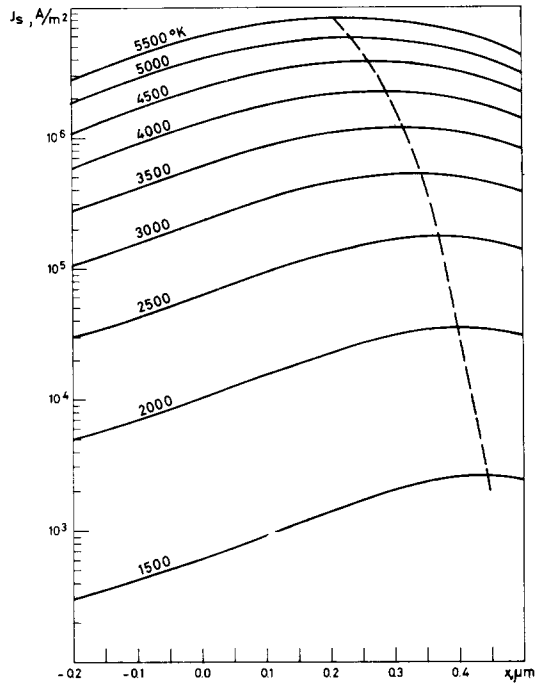

Fig. 7. Current density yield $J_s(A/m^2)$ as function of temperature (°K) and filter passband displacement (μm).

function of temperature for the mirror–filter configurations with $x = 0.0$ and $x = +0.35$ (η_s; *c* & *a*). Also shown are the cases for no mirror (η_0, *f*) and with the idealized, square cut-off mirror (η_I; *e*&*e'*). For each we have included separate curves normalized to remove the variations due to the intensity level on the cell, to illustrate the quantitative effect of the intensity dependent cell characteristics attributed to the data of Fig. 2 and extrapolations. The corresponding set of curves (dashed lines) are the results for constant and identical V_{oc} and *FF* (corresponding to 500 suns) and cancel that effect entirely. It should be noted, in this regard, that with the particular cell characteristics used, the increasing V_{oc} is offset by a decreasing *FF* (contrary to theoretical expectations) so the intensity effects may actually be significantly greater for cells with other designs or improved processing, which should show higher efficiencies at higher intensities.

A single point (η_0^*) is also shown on this figure, corresponding to a modeled AM1 spectrum. The latter is simulated with a 5762K blackbody, modified by experimental molecular atmospheric absorption[14]. Thus the point can be taken as representing a directly used photocell with the EMVJ collection efficiency and with the aforementioned 500 sun V_{oc} and *FF*.

The electrical conversion efficiencies as a function of the *radiation level*, for the filter/emissivity model are shown in Fig. 12, for $x = 0.0$ and $x = 0.35$. Different intensities correspond to different source temperatures as noted. Also shown are the published values[6] achieved under concentrated solar irra-

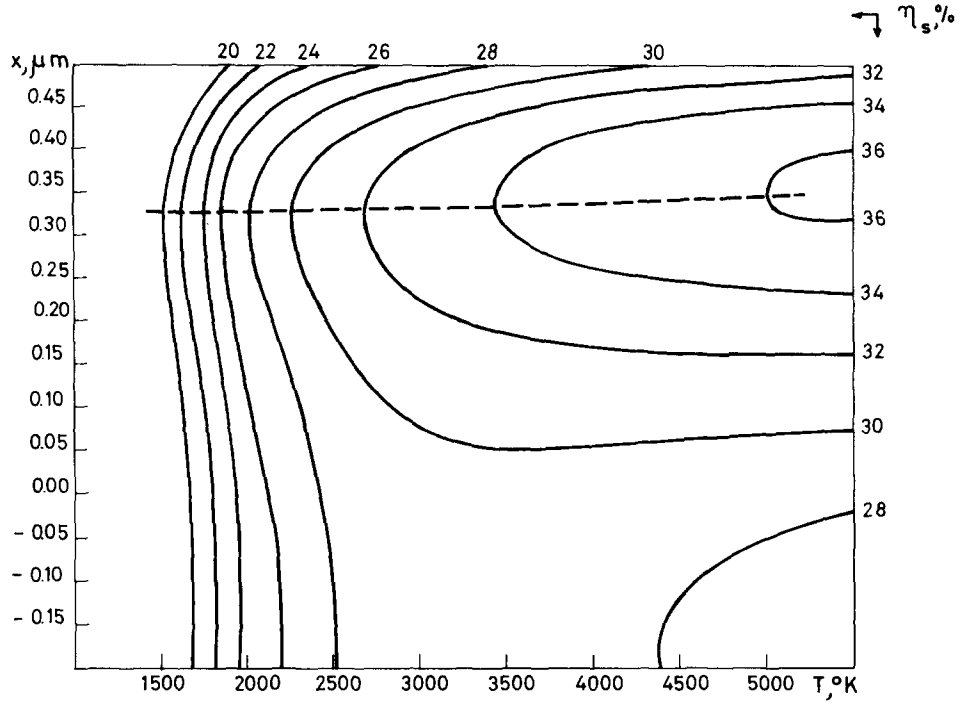

Fig. 8. Electrical efficiency η_s (per cent) as function of temperature (°K) and filter pass band displacement (μm).

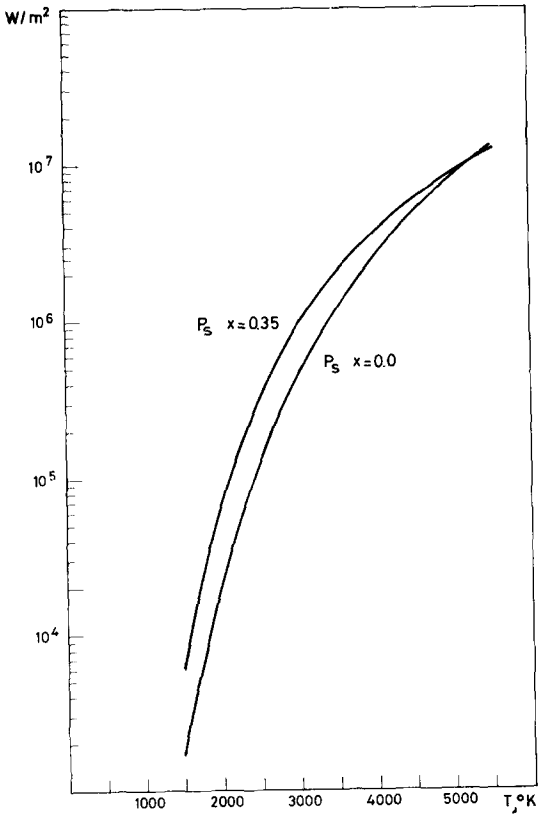

Fig. 9. Light intensity $P_s(W/m^2)$ as a function of temperature (°K) for normal ($x = 0.0$) and reference ($x = 0.35\,\mu$m) passband displacement.

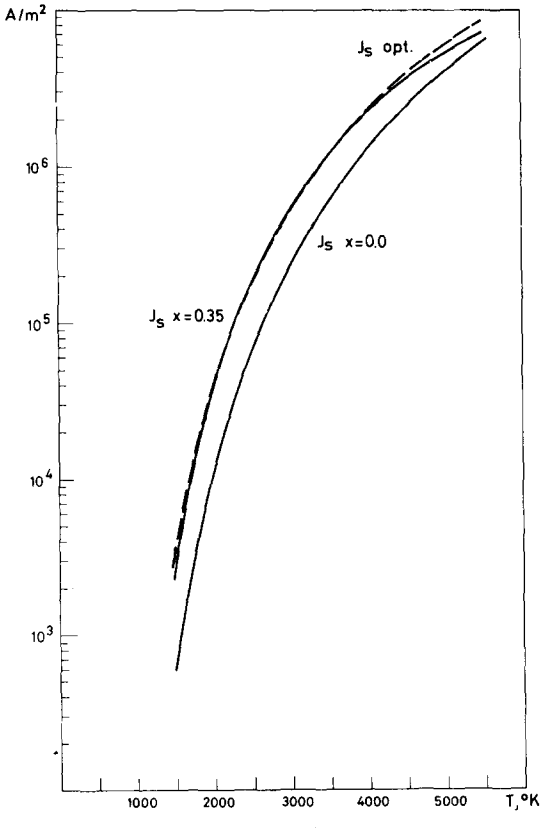

Fig. 10. Current density $J_s(A/m^2)$ as a function of temperature (°K) for normal ($x = 0$) and reference ($x = 0.35\,\mu$m) passband displacement.

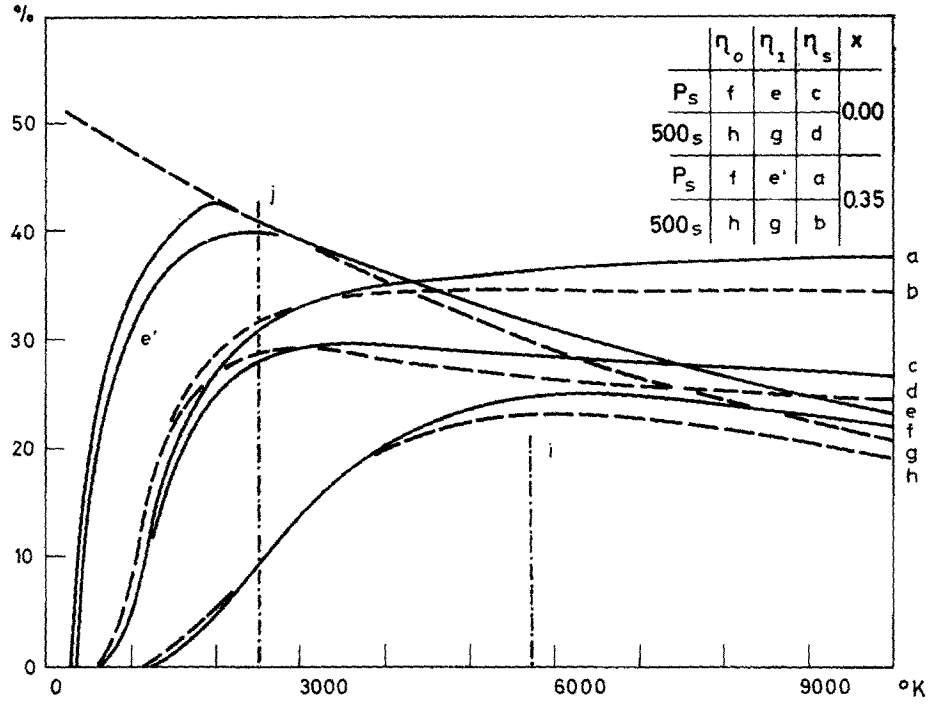

Fig. 11. Electrical efficiencies as a function of temperature (°K); η_0, η_1 and η_s for normal ($x = 0.0\,\mu$m) and reference ($x = 0.35\,\mu$m) passband displacement and for constant and intensity-dependent cell parameters.

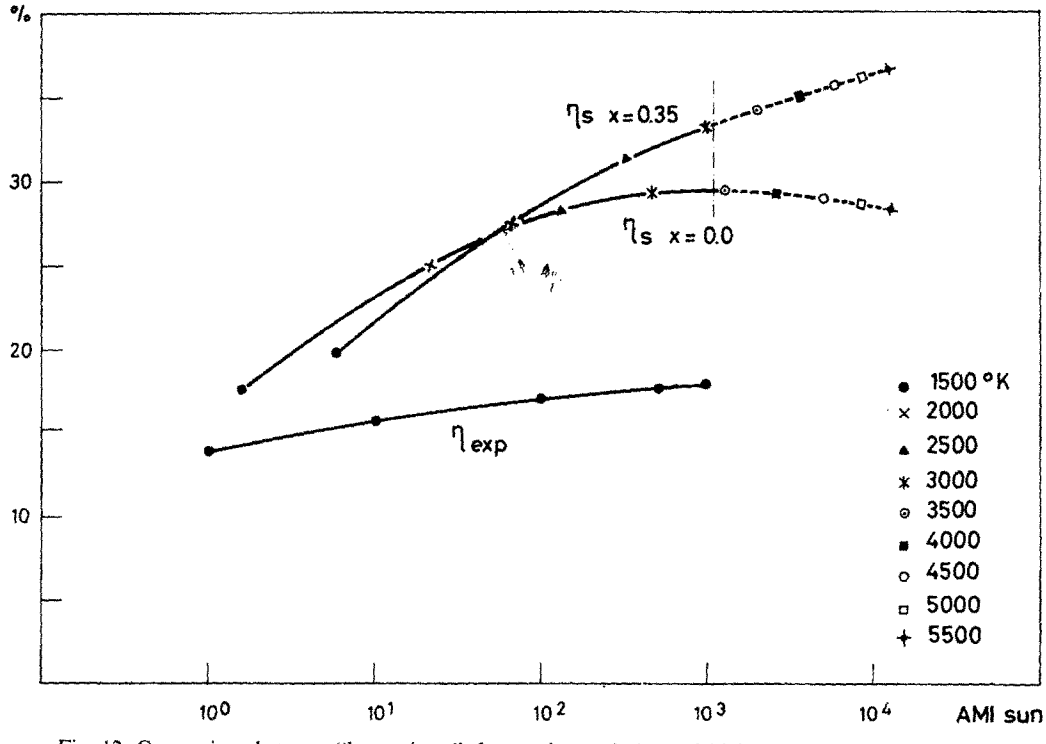

Fig. 12. Comparison between "heat-mirror" thermophotovoltaics and high concentration direct photovoltaics. Efficiencies for the normal ($x = 0$) and reference ($x = 0.35\,\mu$m) sections are shown jointly with experimental data for a high concentration photocell as a function of light intensity. Ref. [6]. η_s values correspond to different source temperatures, as designated.

diation for the EMVJ cell whose other characteristics have been used above.

DISCUSSION

While we have calculated the thermal model system over a larger range of temperature, materials limitations would suggest that the η curves beyond, say, 3000K are not of practical interest. Also, where intensity-dependent cell values have been used in the η estimations it needs to be pointed out that large extrapolations have been made into unexplored intensity regions for the high temperature portions.

Apart from the latter caveat, the η_0 curve can be considered to be a simulation of the direct use of a silicon solar cell with a "sun" of variable temperature, as well as the base model for the thermophotovoltaic systems. (It is presumably only a coincidence that the optimum η_0 source temperature for silicon is near 6000K, the sun's temperature). However, the η_0^* point is more accurate for quantitative comparison with direct use of photocells. The difference between the η_0^* value, 21.3 per cent, and the experimental value, ~18 per cent[6], can be attributed to the presumption of a more effective antireflection coating and to ignoring of any obscured cell surface area; it agrees very well with the expectations from anticipated relevant device improvements[6]. (It might be mentioned, in this context, that for the thermophotovoltaic system much of the incident radiation not transmitted into the cell will return to the source and would not actually worsen the efficiency in the normal sense).

It should be further stressed that apart from some collection efficiency effects, the values for efficiency given here are all relative to the behavior of an actual cell. Thus, for example, if processing changes improve the $V_{oc} \cdot FF$ product of the cell (at a relevant intensity), the thermophotovoltaic output also improves by the same factor. On the other hand, the close coupling between source temperature and radiated intensity level means that it will not be possible to take full benefit of the advantages anticipated from very high intensity levels, such as much smaller cell areas and higher cell efficiency. It would appear to be difficult, for example, to reach or exceed the roughly 3×10^5 W/m^2 (300 suns) of incident radiation calculated for a 2500K source. Keeping these points in mind, the comparison of greatest importance is η_0^* relative to the η_s and η_I values at about 2500K.

It is instructive to consider certain physical factors relating to the calculated values. At low temperature (e.g. 1500K), the radiated power level is low and the fraction of that which is in the useful energy range (e.g. $E > E_{gap}$) is also low; thus high useful intensities are not achieved and large cell areas are needed. Of equal practical concern, with a low temperature source, is the fact that when only a small fraction of the source radiation is directly effective in the conversion process, even tiny non-idealities acting on the remainder can have a large effect on the apparent efficiency. At very high temperatures, extremely high radiation levels would be reached (e.g. 10^7 W/m^2 at 5500K) and a large part of that radiation is at high energy; so much so that much of the energy conversion loss would be due to the second term in eqn (1).

Regarding the η_0 curve, the efficiency is essentially zero at 1500K because so little of the radiation has $E > E_{gap}$. Almost all the energy is lost in the first term of eqn (1). The decrease in η_0 beyond about 6000K arises from the continuing growth of the second term.

The η_I curve would be expected to rise towards 100 per cent efficiency at sufficiently low temperature where the highest energy photon was exactly at E_{gap}. However, at that point the output power would be negligible. The fact that the η_I curve with intensity-dependent photocell parameters actually decreases below 2000K is due to the fall-off in V_{oc} at low intensity (V_{oc} is approximately proportional to ln (intensity)). At higher temperatures the monotonic decrease in η_I is entirely due to the second term in eqn (1). Indeed η_I and η_0 approach congruency when little of the radiation has $E < E_{gap}$ and the "ideal" step-mirror plays no role. This phenomenon is also seen clearly in the crossover with the $\eta_s(x = 0.35)$ and (ultimately) with $\eta_s(x = 0)$ curves. Although certainly less effective for photons with $E < E_g$, the physically plausible $\tau_M(\lambda)\epsilon(\lambda)$ product is more useful than the step filter at high temperature.

In addition to simulating a pseudo-optimization of the heat-mirror configuration of Fig. 1, η_I is also an idealization for rear mirror configuration with a constant source emissivity. As it applies to that situation, η_I simulates the following: radiation reflected at the cell surface is entirely retrieved by the source; radiation absorbed by the cell ($E > E_{gap}$) is converted to electricity with experimental effectiveness (albeit with an idealized $S(\lambda)$); radiation transmitted by the cell (essentially all with $E < E_{gap}$) is reflected back through the cell and retrieved by the source.

The sharper fall-off of the η_s curves at low temperature is due mainly to the fact that some of the low energy radiation ($E < E_{gap}$) is passed by the real heat-mirror and that amount is significant in terms of the useful light available at low temperatures. It is also worth pointing out in that regard, that the wavelength selective emissivity seems to have as its primary benefit the reduction of the long wavelengths just beyond 1.1 μm.

In comparing $\eta_0^* = 21.3$ per cent to η_s ($x = 0.35$, $T = 2500\text{K}) = 31$ per cent and η_I ($T = 2500\text{K}) = 41$ per cent we see the apparent potential for significant gains with the thermophotovoltaic systems. However, for each of the two configurations we have thus far neglected absorption at the mirror. For the rear-mirror configuration, η_I also ignores any photons with $E < E_{gap}$ which are nonetheless absorbed in the cell. Although these are small percentage effects, they act on a major fraction of the total energy and have large negative leverage. They have not been included in the modelling specifically because they can have

large net effects, yet are not known with good precision. We can, however, estimate plausible magnitudes. For the rear mirror situation (η_l), at 2500K, approximately 78 per cent of the emitted radiation will be reflected back to the source. If we assume that the rear mirror has an actual reflectivity of 92 per cent and that absorption in the cell of photons with $E < Eg$ is 2 per cent, we find that for each 100 units of energy radiated from the source, we get approximately 9 units of electricity, and about 20.7 units of heat generated in the cell (13 due to $E > Eg$ losses, 1.5 due to $E < Eg$ absorption and 6.2 at the rear mirror), yielding a net efficiency of 30 per cent. For the heat mirror case (η_s), and the same temperature, approximately 14 per cent of the energy is transmitted to the cells. If the mirror has an absorption of 2 per cent (of the total incident light), for the same source radiance, we get 4.34 units of electricity, 9.66 units of heat in the cell, and 2 units of heat in the front filter mirror, yielding an efficiency of 27 per cent. Thus, it would appear that the two approaches will be comparable in net efficiency, but the first yields more electricity per unit cell area. If we also assume a radiative power loss through the entrance aperture of about 2 per cent, we might expect net efficiencies in the 25–28 per cent range, compared to the η_0^* of 21.3 per cent.

These results, then, are not strongly encouraging for the thermophotovoltaic concepts, but they do point out the specific areas in which improvements in materials properties might be most effective.

NOMENCLATURE

- α absorptivity
- τ transmissivity
- ρ reflectivity
- ϵ emissivity
- λ wavelength
- η efficiency
- J current density
- P light intensity
- S quantum yield
- T temperature
- V_{oc} open circuit voltage
- FF fill factor
- E energy
- E_{gap} energy to create an electron-hole pair
- x passband displacement
- h Planck's constant
- c speed of light
- k Boltzmann's constant
- σ Stefan–Boltzmann's constant
- q charge of electron
- AM1 air mass one
- EMVJ etched multiple vertical junction
- N AM1 solar spectrum of photons
- η_0^* modeled AM1 efficiency for EMVJ cells
- η_{exp} experimental efficiency for EMVJ cells

Subscripts

- M mirror
- AR anti-reflectance
- s modeled heat-mirror
- o ideal, without heat-mirror
- I ideal, with perfect heat-mirror

REFERENCES

1. D. C. White, B. D. Wedlock and J. Blair, Recent advance in thermal energy conversion. Session on thermal energy conversion. *Proc. 15th Ann. Power Sources Conf.*, Atlantic City, New Jersey (1961).
2. B. D. Wedlock, Thermo-photovoltaic energy conversion. *Proc. IEEE* **51**, 694–698 (1963).
3. R. L. Bell, Concentration ratio and efficiency in thermophotovoltaics. *Solar Energy* **23**(3), 203–210 (1979).
4. R. M. Swanson, *Silicon Photovoltaic Cells in TPV Conversion.* Electric Power Research Insititue Report ER-1272, Stanford University (1979).
5. R. I. Frank and Roy Kaplow, Performance of a new high intensity silicon solar cell. *Appl. Phys. Lett.* **34**(1), 65–67 (1979).
6. R. I. Frank, J. L. Goodrich and R. Kaplow, A low series resistance silicon photovoltaic cell for high intensity applications. *14th IEEE Photovol. Spec. Conf.* (1980).
7. F. Reif, *Blackbody Radiation. Fundamentals of Statistical and Thermal Physics.* 9.13-9.14-9.15, 373–388. McGraw-Hill, New York (1965).
8. R. V. Dunkle, Thermal-radiation tables and applications. *Trans. ASME*, pp. 549–552 (1954).
9. J. A. Duffie and W. A. Backman, *Solar Energy Thermal Processes*, pp. 64–71. Wiley, New York (1974).
10. J. C. C. Fan, F. J. Bachner, G. H. Foley and P. M. Zavracky, Transparent heat-mirror films of $TiO_2/Ag/TiO_2$ for solar energy collection and radiation insulation. *Appl. Phys. Lett.* **25**(12), 693–695 (1974).
11. A. Musset and A. Thelen, *Progress in Optics* (Edited by E. Wolf), Chap. 4. North-Holland, Amsterdam (1970).
12. H. J. Hovel, Solar cells. In *Semiconductors and Semimetals*, Vol. 11. New York, Academic Press (1975).
13. D. P. DeWitt and Y. S. Touloukian, *Thermal Radiative Properties of Nonmetallic Solids.* Vol. 8, p. 184. IFI Plenum, The TPRC Data Series, Thermo-Physical Properties of Matter. New York–Washington (1972).